Nano-Photonic Crystal Waveguides for Ultra-Compact Tunable True Time Delay Lines

YongQiang Jiang[1], Wei Jiang[2], Xiaonan Chen[1], Lanlan Gu[1], Brie Howley[1], Ray T. Chen[1]*

1. Microelectronic Research Center, Department of Electrical and Computer Engineering, The University of Texas at Austin, Austin, TX 78758, USA
* Email: chen@ece.utexas.edu
2. Omega Optics Inc., Austin, TX 78758, USA

ABSTRACT

Nanophotonics including photonic crystals promises to have a revolutionary impact on the landscape of photonics technology. Photonic crystal line defect waveguides show high group velocity dispersion and slow photon effect near transmission band edge. By using photonic crystal waveguides to build true time delay based phased array antenna or other optical signal processing systems, the length of the tunable true time delay lines can be dramatically reduced inversely proportional to group velocity dispersion in dispersion enhanced system architecture or reduced inversely proportional to group index in slow photon enhanced system architecture. The group index of the fabricated silicon photonic crystal line defect waveguide is experimentally demonstrated as high as 40 at optical wavelength around 1569 nm. The group velocity dispersion of the fabricated silicon photonic crystal line defect waveguide is as high as 50 ps/nm·mm at wavelength around 1569 nm, which is more than 10^7 times the dispersion of the standard telecom fiber (D = 3 ps/nm·km). Due to the integration nature of photonic crystals, system-on-chip integration of the true time delay modules can be easily achieved.

Keywords: Photonic crystal waveguide, phased array antenna (PAA), optical true time delay (TTD), group velocity dispersion (GVD), slow photon, wavelength tuning

I. INTRODUCTION

Phased array antennas (PAAs) have the advantages of high directivity and quick beam steering without physical movement. Each antenna element of a PAA must have the correct phase condition to accomplish the desired beam steering, as shown in Fig. 1. However, the conventional electrical phase trimmer technique is intrinsically narrow-band and introduces beam squint, which means that the radiating beam changes direction when the microwave frequency changes. Recently, there has been growing interest in optical true time delay (TTD) techniques with the features of wide bandwidth, compact size, reduced system weight, and low electromagnetic interference when compared with electrical TTD techniques [1-2]. The optical TTD techniques can be used not only in PAA systems, but also in other optical signal processing systems [3-4]. However, most of the optical TTD techniques require a large number of precisely time-delay matched optical elements such as lasers and optical delay segments resulting in a complex system design. Esman et al proposed a fiber-optic TTD technique using conventional dispersion compensating fiber (D = -100 ps/nm·km) to meet these requirements [2]. However, its dispersion parameter D of is fairly small, thus long fibers are still needed in the TTD module to get the required time delay. Jiang et al recently demonstrated a dispersion enhanced wavelength tunable TTD technique for an X-band phased array antenna using dispersion enhanced photonic

Photonic Crystal Materials and Devices III, edited by Ali Adibi, Shawn-Yu Lin, Axel Scherer,
Proc. of SPIE Vol. 5733 (SPIE, Bellingham, WA, 2005) · 0277-786X/05/$15 · doi: 10.1117/12.588735

crystal fiber (D = -600 ps/nm·km) to shorten the delay line length [5]. If the delay line group velocity dispersion is increased, the total delay line length will be decreased proportionally.

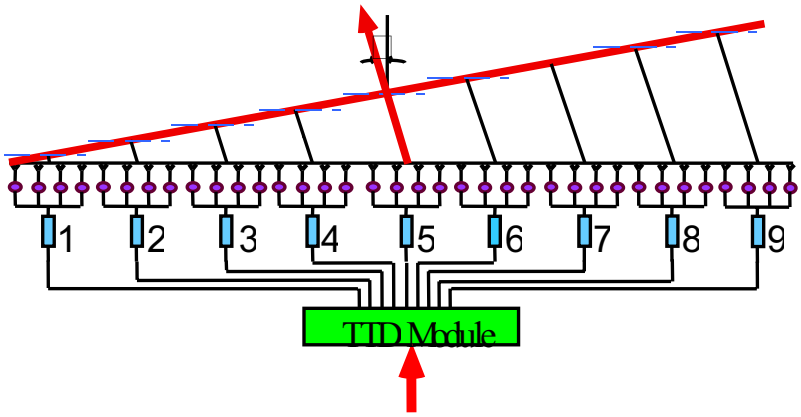

Fig.1. Schematic diagram of true time delay based phased array antenna system.

At the same time, photonic crystals (PhCs) have become a hot topic since 1990's. Nanophotonics including PhCs promises to have a revolutionary impact on the landscape of photonics technology. Photonic crystals are a new class of artificial optical materials with periodic dielectric structures, which result in unusual optical properties and promise to provide revolutionary solutions to the miniaturization of photonic devices. Photonic crystals with photonic band gaps (PBGs) are expected to be key platforms for future optical integrated circuits [6-8]. Due to its unique properties, the size of most optical components can be greatly reduced. In initial studies it seems that 3-D PhC structures with 3-D PBGs are essentially required to obtain these unique properties. However, recent studies show that 2-D PhC slab can also obtain very good performance [9]. PhC slabs are 2-D PhC structures located within the slab waveguide. In PhC slab, the light is confined by a combination of in-plane PBG confinement and vertical total-internal-reflection (TIR) confinement. One simple way to utilize the PBG effect is to introduce functional defects into PhCs, which is analogous to doping intentional defects in electronic crystals to introduce defect bands. Line defects can work as strongly confined waveguides. Due to all these unique properties and easy fabrication techniques, 2-D PhC slab line defect waveguides have been most extensively studied [9-13].

One of the most interesting and exciting properties is high group velocity dispersion and slow photon effect near transmission band edge. Notomi et al firstly demonstrated high group velocity dispersion and slow photon defect using silicon photonic crystal waveguide [10]. Several other groups also demonstrated this effect in both line defect and coupled cavity photonic crystal waveguide [14-17]. Insertion loss including propagation and coupling loss is also a very import factor for using these waveguide. Kuramochi et al demonstrated 0.5 dB/mm on silicon photonic crystal waveguide [18]. Barclay et al demonstrated 94% coupling efficiency by evanescent coupling between a silica optical fiber and a silicon PhC waveguide [19]. The total insertion loss is low enough for most practical application.

In this letter, we propose two novel optical true time delay (TTD) architectures using an array of highly dispersive PhC waveguides. The highly dispersive PhC waveguides are designed, fabricated and characterized. The TTD modules are based on highly dispersive PhC waveguides reported herein and other non-dispersive waveguides. The TTD modules are potentially ultra-compact and system-on-chip compared with bulk fibers and other photonic TTD techniques.

II. DESIGN OF PHOTONIC CRYSTAL WAVEGUIDES

We use a W-1 line defect PhC waveguide design to achieve high group velocity dispersion or slow photon effect (high group index). The W-1 line defect photonic crystal waveguide can be easily generated by removing a single line defect from pure 2-D photonic crystal slab, as shown in Fig. 2. The slab is generated on a silicon-on-insulator wafer. The thickness of the silicon core layer is t = 220 *nm*. Top cladding is air and bottom cladding is buried oxide layer with thickness of 2 μm. The pitch size of the PhC is a = *400 nm*. The normalized air hole diameter is d/a = 0.55. The dispersion diagram of PhC waveguides can be calculated using the 3-D full vectorial plane-wave expansion (PWE) method, which is fast and accurate compared to other methods [20]. Since our PhC waveguide design is a 2-D PhC slab with line defects, we need to use a supercell having a size of N×M×L instead of a natural unit cell to implement the periodic boundary conditions. As shown in Fig. 2 a 7×1×5 supercell is used for simulation purposes. The simulated electrical and magnetic field intensities, $|E|^2$ and $|H|^2$, are also shown in Fig. 2. It shows that most of energy is guided around the defect inside the supercell. More simulation is done on the PhC waveguide. We can clearly see that the guided mode around the line defects, as shown in Fig. 3. We should notice here that normalized by the maximum intensity of the guided mode at the vertical center of the silicon slab waveguide at Y = 0, the maximum intensity at Y = 54.8 nm is less than that at Y = -54.8 nm. The reason is that the guided mode decays faster in the top air layer than in the bottom buried oxide layer.

The dispersion parameter, ω(k), of PhC waveguide described above is also shown in Fig. 4(a). The bandgap is located between normalized frequencies a/λ = 0.245 ~ 0.300. The guided mode in the bandgap generated by introducing line defect is clearly shown here. The derived group index versus free-space optical wavelength is shown in Fig. 4(b). The large group index n_g = 60 is obtained around 1546 nm in this structure. The group index changes rapidly around the transmission band edge, which means high group velocity dispersion. The reason behind is due to the unusual flat of the guided mode around the transmission band edge in the dispersion diagram which leads to small group velocity thus high group index and large group velocity dispersion.

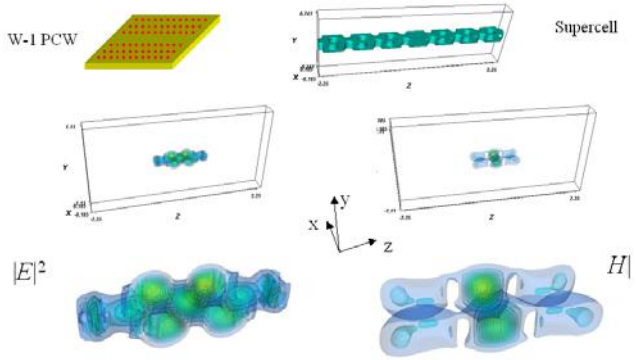

Fig. 2. Photonic crystal waveguide W-1 line defect schematic diagram, supercell used in simulation by 3-D full vectorial plane wave expansion method and electrical and magnetic filed intensity from the simulation.

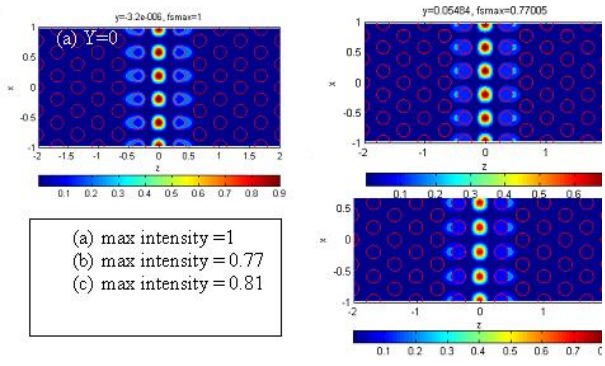

Fig. 3. Simulation of guided mode by 3-D full vectorial plane wave expansion method.

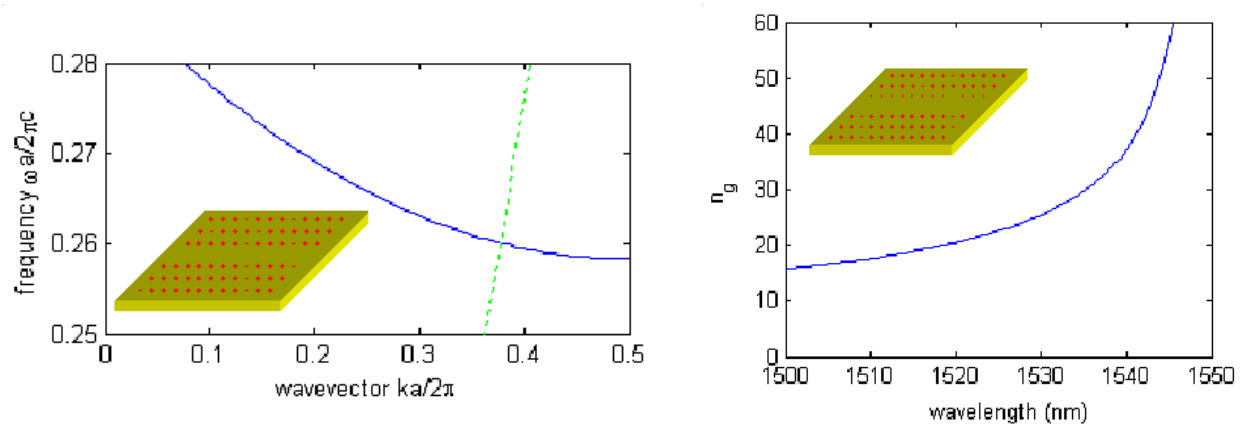

Fig. 4. (a) Dispersion diagram of a W-1 line defect photonic crystal slab waveguide by 3-D full vectorial plane wave expansion method. (b) Derived group index versus wavelength from dispersion diagram. High group index and large group velocity dispersion are clearly shown near transmission band edge at 1546 nm.

III. FABRICATION OF PHOTONIC CRYSTAL WAVEGUIDES

We fabricated photonic crystal waveguides (PCW) with silicon-on-insulator (SOI) based hexagonal periodic air-hole structures. We typically start with wet growing about 60 nm oxide at 850°C on top of a 6" SOI wafer. Then we cut it into about 1 cm × 1cm square pieces. First PhC structures are patterned with E-beam resist ZEP-520A by E-beam nano-lithography (JEOL JBX-6000FS/E, resolution: 20 nm). After resist developing, the patterns are transferred to 60 nm oxide mask layer by CHF_3 chemistry in RIE. Then the E-beam resist residue is removed by plasma ashing in O_2. Finally the patterns are transferred to silicon core layer with oxide as the mask layer by HBr and Cl_2 chemistry in RIE. On each chip, devices with lattice constant a = 400 nm, air hole diameter d = 220 nm, and slab thickness t = 220 nm are fabricated. Post-etching oxidation at 850° is implemented for about 1 minute. The post-etching oxidation forms an additional 6~7nm oxide layer, with a surface significantly smoother than the original silicon surface after the dry etching. The air holes of the silicon photonic crystals expand noticeably after the completing the entire fabrication sequence. E-beam resist exposure and development, dry-etching of the oxide hard mask and the SOI layer all incur certain amount of expansion of the holes. Dry-etching SOI layer appears to be the most critical step in hole size control. We have optimized the process parameters and have introduced a proper pre-offset of the hole size in e-beam pattern design so that the hole size can be controlled with an accuracy of 5%.

IV. CHARACTERIZATION OF PHOTONIC CRYSTAL WAVEGUIDES

1. Morphological examination

The nano-structures of silicon photonic crystal waveguide have been imaged by a FEI Strata DM235 SEM/FIB nano-characterization. A number of scanning electron microscopic (SEM) pictures are shown in Fig. 5(a), which demonstrates the high quality of the silicon nano-structures fabricated through our optimized processes. For reference, we show in Fig. 5(b) an early fabrication result where the post-etching oxidation was not employed. In addition, we have

also used the focus ion beam (FIB) to polish the end-face of silicon rib waveguides. The resultant smooth end-face, as illustrated in Fig. 5(c) helps reduce the coupling loss between the silicon rib waveguide and the input fiber.

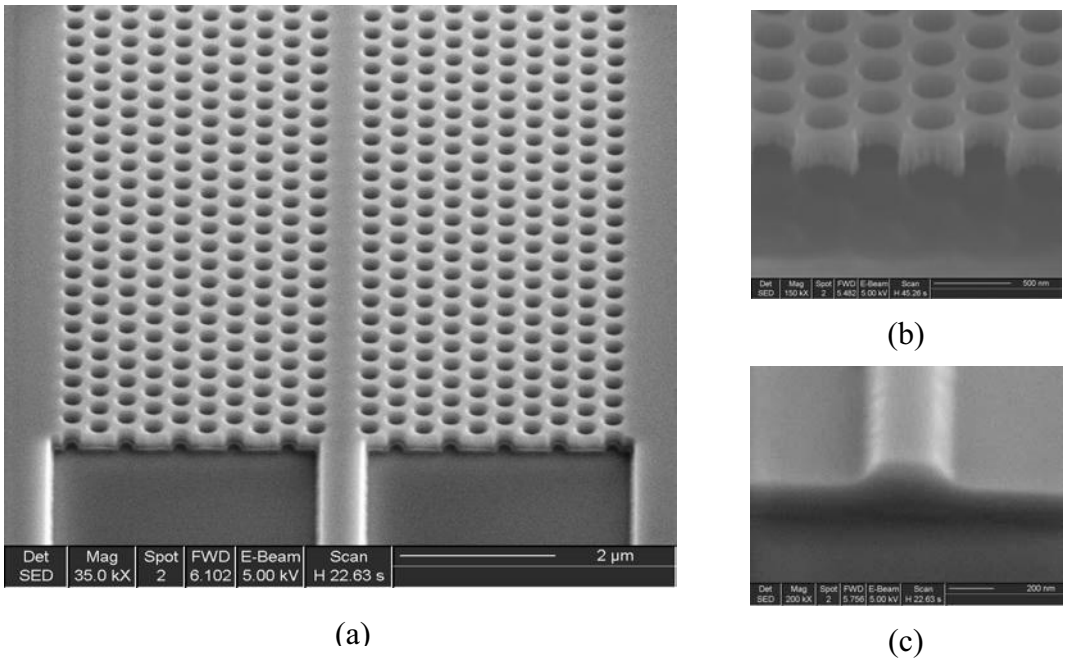

Fig. 5 SEM pictures of the nano-structures of silicon photonic crystal waveguides. (a) PCW fabricated *with post-etching oxidation*. The waveguide is based on a triangular lattice with lattice constant a=400nm, hole diameter d=210nm, and SOI thickness t=215nm. (b) Photonic crystal sidewall profile when the post-etching oxidation is NOT performed. The surface roughness is evident. (c) The silicon rib waveguide end-face polished by focus ion beam (FIB); highly smooth surface facilitates coupling.

2. Measurement of optical transmission

We also accurately characterize the optical transmission and dispersion of photonic crystal waveguide modes. A simplistic approach places a PhC waveguide between two straight silicon rib waveguides. However, the stray light—light reaching the output through the air above the chip surface—in the forward direction is often strong enough to smear the signal transmitted via the rib-PCW-rib guided channel. To overcome this problem, we introduced a waveguide bend [21], which shifts the output fiber by at least 600µm and significantly suppresses the stray light collected by the output fiber. The measurement illustrated in Fig. 6 is performed on a fully automated Newport Photonics Alignment/Packaging Station. Two lensed fibers are manipulated by two automated 5-axis stages, which are controlled by a computer to precisely align the fibers with the rib waveguides. Figure 7(a) shows a typical transmission spectrum of PhC waveguide with length 100a, which is normalized by the spectrum of a silicon rib waveguide (with the same bend and length). Below 1560nm, a guided mode is present in the gap. The bulge in the longer wavelength part of the spectrum is attributed to the lower band of the photonic crystal.

A 40μm-long PCW has typical loss of 6.5±2dB, while a 320μm-long PCW has typical loss of 8.3±3dB. From these, one can estimate the propagation loss is fairly low, about 6.4dB/mm. The coupling loss at each interface between a PCW and a Si rib waveguide is about 3.1dB. Note that the waveguides fabricated without post-etching oxidation [Fig. 5(b)] typically have propagation losses over 20dB/mm, which manifests the advantage of oxidation.

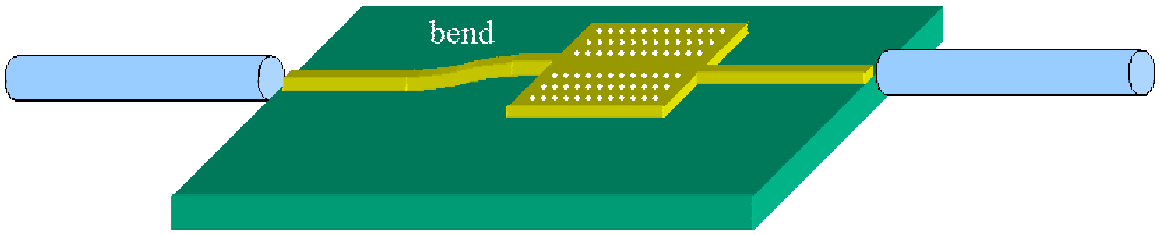

Fig. 6. Test setup for measuring the optical transmission of a photonic crystal waveguide. Two lensed fibers are used for better mode matching. A waveguide bend is used to shunt the relatively intense stray light in the forward direction.

3. Group index and group velocity dispersion calculation

The group index $n_g=c/v_g$ is calculated *directly* from the varying Fabry-Perot oscillation period of transmission spectrum [10], which incurs high uncertainty and fluctuation of computed n_g values due to noise and finite wavelength resolution of the spectrum. Similar problems occur in analyzing signals such digitized human voice, and the countermeasures are well established. Here we introduced a simple Windowed Fourier Transform (WFT) algorithm [22], which computes n_g from experimental transmission spectra with low fluctuation. Figure 7(b) attests the high n_g as anticipated, which promises over 10 times reduction in delay line length. The group velocity dispersion is also calculated as 50 ps/nm·mm at 1569 nm. The dispersion is increased by 10^7 times compared to standard telecom LEAF fiber that has a dispersion parameter of 3 ps/nm·km.

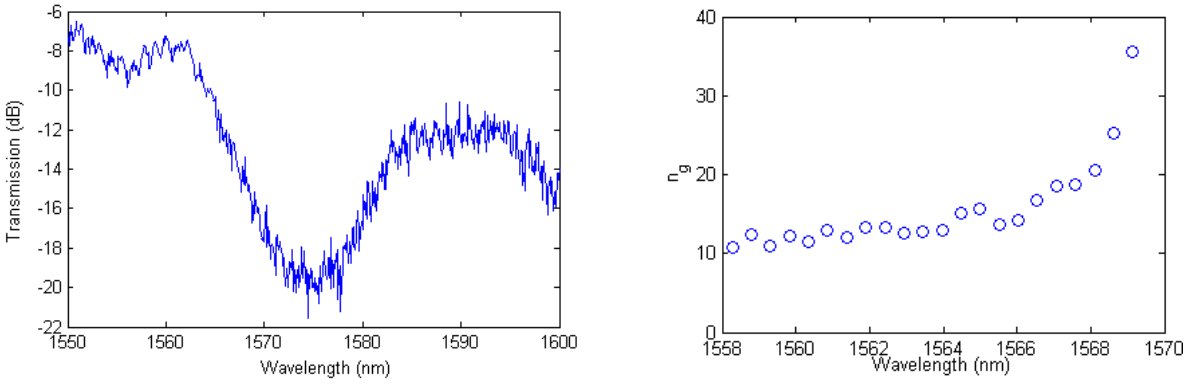

Fig. 7 (a) Transmission spectrum for a PCW with length 100a = 40μm, normalized by the spectrum of a Si rib waveguide. (b) Group index n_g for a PCW, salient increases of n_g is evident..

V. TTD BASED ON PHC WAVEGUIDES

Line defect photonic crystal waveguides show high group velocity dispersion and slow photon effect as shown above. We proposed two TTD system architectures using the fabricated highly dispersive PhC waveguide delay lines mentioned above. These are *dispersion enhanced wavelength tunable TTD architecture* and *slow photon enhanced reconfigurable TTD architecture*. By using photonic crystal waveguide to build true time delay based phased array antenna, the TTD payload can be reduced inversely proportional to group velocity dispersion in dispersion enhanced system architecture or inversely proportional to group index in slow photon enhanced system architecture.

1. Dispersion enhanced wavelength tunable TTD architecture

In dispersion enhanced wavelength tunable TTD architecture, the lengths of the highly dispersive PhC waveguides are *L*, *L*(n-1)/n*, *L*(n-2)/n*, …, *L*2/n*, *L/n*, and *0*, as shown in Fig. 8(a). Theses PhC waveguides are connected to non-dispersive waveguide with lengths *0*, *L/n*, *L*2/n*, …, *L*(n-2)/n*, *L*(n-1)/n*, *L*, respectively. This would make the total length of each delay line *L*. Each delay line has the same nominal group delay at the central tuning wavelength λ_o but with slightly different net dispersion by slight trimming the lengths of the non-dispersive waveguide or the connected optical fiber. The relative delay of the signals among the delay lines can thus be changed by tuning the optical wavelength. At the central tuning wavelength λ_o, all the time delays are matched by trimming the non-dispersive waveguide. Thus, at λ_o the main antenna beam will be directed broadside. At wavelengths deviating from λ_o, each of the delay lines generates a time delay proportional to its dispersion parameter, D, and the highly dispersive PhC waveguide length, resulting in a phase change to steer the main antenna radiation beam. [2]

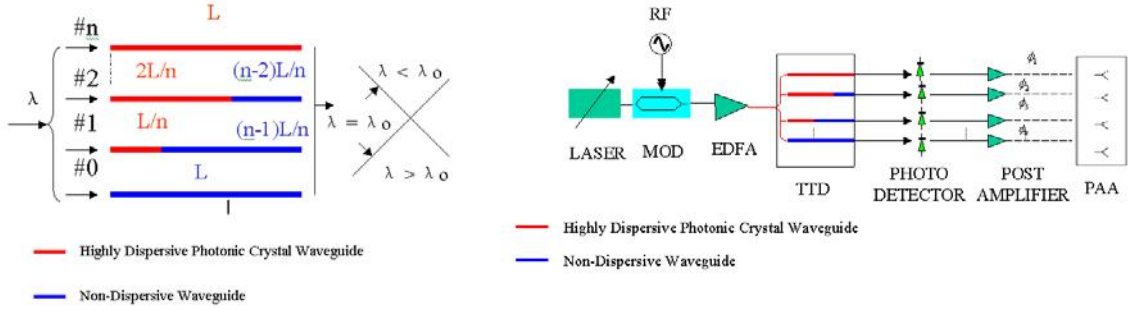

Fig. 8. (a) Dispersion enhanced wavelength tunable true time delay architecture. (b) Dispersion enhanced wavelength tunable true time delay for phased array antenna system setup.

A proposed 1-D system diagram using the proposed dispersion enhanced wavelength tunable TTD architecture is shown in Fig. 8(b), which is similar to the work demonstrated by Jiang et al [5]. An *N*-element 1-D X-band PAA system is proposed. A microwave signal is generated from the HP network analyzer 8510C [5]. The optical carrier from a tunable laser (tuning range: 1520-1580nm, spectral width: 200MHz, tuning resolution: <0.024nm) is modulated by a 10Gb/s $LiNiO_3$ modulator, optically amplified by an erbium doped fiber amplifier (EDFA), then distributed into the *N* sub-units of the TTD delay lines by a one-to-*N* fiber splitter. After the pre-determined time delay, the optical signals with correct phase relationships are detected by InGaAs high-speed photodiodes (bandwidth: 18 GHz) and individually fed into *N* antenna

elements after electrical amplification. The microwave radiations signals are detected by a microwave receiving horn connected to microwave spectra analyzer (MSA). The computer controlled rotational stage under the antenna head can rotate the antenna to measure the antenna radiation far field pattern. We also need to mention that the ultimate application of this approach is also limited by the tuning speed of the tunable laser. Wipiejewski et al reports a tunable laser with 40ns tuning speed, which is fast enough for most PAA applications [23].

2. Slow photon enhanced reconfigurable TTD architecture

We also proposed a monolithic slow photon enhanced reconfigurable TTD architecture. Reconfigurability of the time delay was built into the structure by combining the PhC waveguides and optical switch [24], as shown in Fig. 9. The optical switch can also be implemented with a PhC approach in the near future [25]. The inclusion of optical switches is critical for application where power-consumption is a sensitive issue. Another advantage of using optical switch is the establishment of the scaling architecture with a minimum number of hardware devices. For example, we can achieve 2^N = 512 time delays with N=9 segment waveguide. The differential time delay through one reconfigurable time delay line τ is proportional to the length and group index. By increasing the group index, the PhC delay line length can be reduced proportionally. Due to the integration of PhC integration, optical integrated circuits can be implemented for this structure.

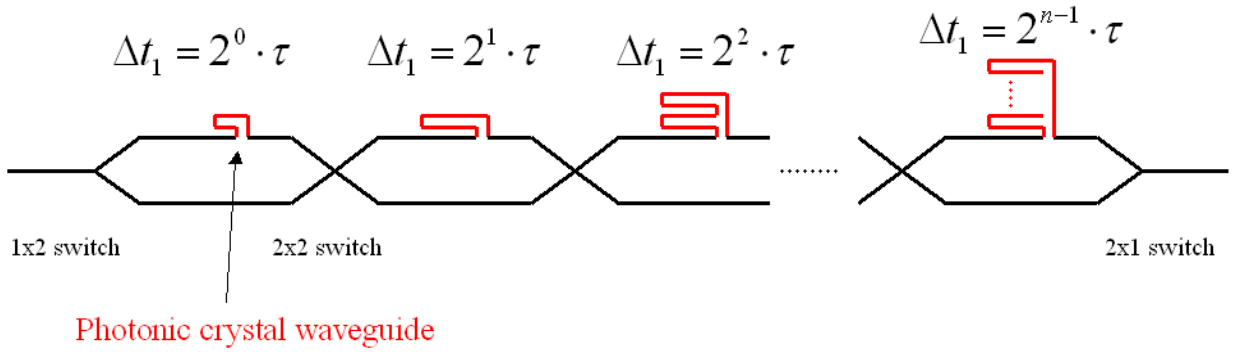

Fig. 9. Slow photon enhanced reconfigurable true time delay architecture.

VI. CONCLUSION

Photonic crystal line defect waveguides show high group velocity dispersion and slow photon effect near transmission band edge. By using photonic crystal waveguides to build true time delay based phased array, the length of the tunable true time delay lines can be dramatically reduced inversely proportional to group velocity dispersion in dispersion enhanced system architecture or reduced inversely proportional to group index in slow photon enhanced system architecture. The group index of the fabricated silicon photonic crystal line defect waveguide is experimentally demonstrated as high as 40 at optical wavelength around 1569 nm. The group velocity dispersion of the fabricated silicon photonic crystal line defect waveguide is as high as 50 ps/nm·mm at wavelength around 1569 nm, which is more than 10^7 times the dispersion of the standard telecom fiber (D = 3 ps/nm·km). Due to the integration nature of photonic crystals, system-on-chip ultra-compact integration of the true time delay modules can be easily achieved.

The system demonstration of highly dispersive silicon photonic crystal waveguides based true time delay for phased array antenna is on going now and will be presented in the near future.

ACKNOWLEDGMENT

This work is supported by Air Force Office of Scientific Research (AFOSR). We thank the Center for Nano and Molecular Science and Technology at the University of Texas at Austin, Welch Foundation and SPRING for partial support of Dual Beam FIB/SEM usage. We also thank Dr. J. R. Cao of University of Southern California and Dr. B.R. Miao of University of Delaware at for fruitful discussions.

REFERENCES

[1] W. Ng, A. A. Walston, G. L. Tangonan, etc, "The first demonstration of an optically steered microwave phased array antenna using true-time-delay," IEEE Journal of Lightwave Technology, vol. 9, pp. 1124, 1991

[2] R. D. Esman, M. Y. Frankel, J. L. Dexter, etc., "Fiber-optic prism true time-delay antenna feed", IEEE Photonics Technology Letter, vol. 11, pp. 1347, 1993

[3] X.S. Yao, L. Maleki, "A novel 2-D programmable photonic time-delay device for millimeter-wave signal processing applications", IEEE Photonics Technology Letters, vol. 6, pp. 1463, 1994

[4] R. A. Minasian, "Photonic signal processing of high-speed signals using fibre gratings", International Topical Meeting on Microwave Photonics, 17-19 Nov. 1999 Pages:219 - 222 vol.1

[5] Y.Q. Jiang, B. Howley, Z. Shi, "Dispersion-Enhanced Photonic Crystal Fiber Array for a True Time-Delay Structured X-Band Phased Array Antenna", IEEE Photonic Technology Letters, vol. 17, pp. 187-189, 2005

[6] E. Yablonovitch, "Inhibited spontaneous emission in solid-state physics and electronics", Phys. Rev. Lett., vol. 58, pp. 2059-2062, 1987

[7] S. John, "Strong localization of photons in certain disordered dielectric superlattices", Phys. Rev. Lett., vol. 58, pp. 2486-2489, 1987

[8] J.D. Joannopoulos, R.D. Meade, J.N. Winn, Photonic Crystals, Princeton University Press, 1995

[9] S.G. Johnson, S. Fan, P.R. Vileneuve, J.D. Joannopoulos, L.A. Kolodziejski, "Guided modes in photonic-crystal slabs," Phys. Rev. B, vol. 60, pp. 5751-5780, 1999

[10] M. Notomi, K. Yamada, A. Shinya, J. Takahashi, C. Takahashi, I. Yokohama, "Extremely large group velocity dispersion of line-defect waveguide in photonic crystal slabs", Phys. Rev. Lett., vol. 87, pp. 253902, 2001

[11] M. Notomi, A. Shinya, S. Mitsugi, E. Kuramochi, H-Y. Ryu, "Waveguides, resonators and their coupled elements in photonic crystal slabs", Optics Express, vol. 12, pp. 1551-1561, 2004

[12] T. Baba, D. Mori, K. Inoshita, Y. Kuroki, "Light localizations in photonic crystal line defect waveguides", IEEE Journal of Selected Topics in Quantum Electronics, vol. 10, pp. 484 – 491, 2004

[13] B.L. Miao, C.H. Chen, S.Y. Shi, J. Murakowski, D. W. Prather, “High-efficiency broad-band transmission through a double-60^{o} bend in a planar photonic Crystal single-line defect waveguide”, IEEE Photonics Technology Letters, vol. 16, pp. 2469-2471, 2004
[14] T. Asano, K. Kiyota, D. Kumamoto, B.S. Song, S. Noda, “Time-domain measurement of picosecond light-pulse propagation in a two-dimensional photonic crystal-slab waveguide”, App. Phys. Lett., vol. 84, 4690-4692, 2004
[15] D. Mori, T. Baba, “Dispersion-controlled optical group delay by chirped photonic crystal waveguides”, App. Phys. Lett., vol. 85, pp. 1101-1103, 2004
[16] T.J. Karle, Y.J. Chai, C.N. Morgan, I.H. White, T.F. Krauss, “Observation of pulse compression in photonic crystal coupled cavity waveguide”, Journal of lightwave technology, vol. 22, pp. 514-519, 2004
[17] M. Soljacic, J.D. Joannopoulos, “Enhancement of nonlinear effects using photonic crystals”, Nature materials, vol. 3, pp. 211-219, 2004
[18] E. Kuramochi, S. Hughes, T. Watanabe, L. Rumunno, A. Shinya, M. Notomi, “Low loss photonic crystal slab waveguides: fabrication, experiment, and theory”**,** LEOS Annual Meeting, vol. 2, pp. 505 – 506, 2004
[19] P.E. Barclay, K. Srinivasan, M. Borselli, O. Painter, “Efficient input and output fiber coupling to a photonic crystal waveguide”, Optics Letters, vol. 29, pp. 697-699, 2004
[20] S. G. Johnson and J. D. Joannopoulos, "Block-iterative frequency-domain methods for Maxwell's equations in a planewave basis," *Optics Express* **8**, pp.173-190, 2001
[21] M. Zelsmann, E. Picard, T. Charvolin, et al, **“**Broadband optical characterization and modeling of photonic crystal waveguides for silicon optical interconnects”, J. Appl. Phys., vol. 95, pp. 1606-1608, 2004
[22] A. V. Oppenheim, R. W. Schafer, Digital signal processing, Prentice-Hall, Upper Saddle River, 1975.
[23] Y. Wipiejewski, Akulova Y.A., Schow C., “Monolithic Integration of a widely tunable laser diode with a high speed electro absorption modulator”, Electronic Components and Technology Conference 2002, pp. 558-562
[24] Y.H. Chen, K. Wu, F. Zhao, R.T. Chen, “Loss compensated photonic true-time-delay for phased array antenna”, IEEE Antennas and Propagation Society Symposium, vol. 14, pp. 4324 – 4327, 2004
[25] Y. Sugimoto, H. Nakamura, Y. Tanaka, N. Ikeda, K. Asakawa, and K. Inoue, "High-precision optical interference in Mach-Zehnder-type photonic crystal waveguide," Opt. Express, vol. 13, pp. 96-105, 2005